

Optical constants change in $\text{As}_{40}\text{Se}_{60}$ and $\text{As}_{50}\text{Se}_{50}$: A comparative study by FTIR and XPS

Ramakanta Naik^{*1}, C. Sripan², R. Ganesan²

¹Department of Physics, Utkal University, Bhubaneswar, 751004, India

²Department of Physics, Indian Institute of Science, Bangalore, 560012, India

*Corresponding author

DOI: 10.5185/amp.2018/6529

www.vbripress.com/amp

Abstract

In this manuscript, the $\text{As}_{40}\text{Se}_{60}$ and $\text{As}_{50}\text{Se}_{50}$ samples of 800nm thickness were deposited onto glass substrate by thermal evaporation technique. The as-deposited films were characterized using X-ray diffraction (XRD) and FTIR Spectrophotometer. The prepared samples are amorphous type. The transmission is found to be decreased for $\text{As}_{50}\text{Se}_{50}$ film. The indirect optical transition mechanism for the photon absorption happens inside the studied film. The optical band gap is decreased with change in As and Se content. The density of state model and increase in disorder is responsible for the reduction of optical band gap in the studied films. The addition of more % As creates localised states in the gap which results the tailing of the band edges. The Urbach energy which gives the degree of disorder changes that indicates the more disorderness of $\text{As}_{50}\text{Se}_{50}$ than $\text{As}_{40}\text{Se}_{60}$ film. The XPS As3d, Se3d core level spectra variation infers the optical changes in the film and such type of film can be used for optical materials and optoelectronics. Copyright © 2018 VBRI Press.

Keywords: Amorphous semiconductor, chalcogenide, thin film, optical property, band gap, XPS.

Introduction

The peculiar properties of chalcogenides affects the structural, optical and photo induced effects that brings these films into applications in solid state devices, nanotechnology, optoelectronics etc. [1-4]. These films have unique properties like high refractive index and large transparency in infrared regions of the energy spectrum, for which they are useful for various applications [5]. The doping of metal impurities changes their properties due to which chalcogenides emerged as multipurpose materials [6,7]. The chalcogenide glasses based on Se has potential applications like optical memory device, switching elements, xerographic applications, rectifiers, photocells, etc. [8]. Se has a disadvantage that its life time is very short and it has low sensitivity. To eliminate this drawback, it is essential to add a metal elements into the selenium matrix. Metal chalcogenide semiconductors based on group V-VI have interesting optical characteristics and have potential for the use in photoelectric, optoelectronic and thermoelectric devices [9,10]. The system based on As₂Se₃ is one of the most studied compound [11] which has potential applications in photonic crystal fiber, watt level super continuum generation etc. [12,13]. Among these, two most important compositions are $\text{As}_{40}\text{Se}_{60}$ and $\text{As}_{50}\text{Se}_{50}$. These types of films have more no defects which are very important for photo induced metastable effects that

occurs at near band gap laser irradiation [14,15]. The symmetric $\text{As}_{50}\text{Se}_{50}$ has an important effect called as opto-mechanical effect [16] which is important for making holographic media, electrochemical sensors, optical gratings, microlenses, nonlinear optical elements, optical memories and photo-resists [17,18].

The optical properties of the chalcogenides play a pivotal role in technological and industrial applications [19,20]. The most important parameter optical band gap has a key role for device fabrication at a particular wavelength. The other optical constants like extinction coefficient (k), absorption coefficient (α) and Urbach energy E_u are important parameters which are calculated from the transmission data by various methods [21,22].

In the present communication, we have investigated the optical properties change in $\text{As}_{40}\text{Se}_{60}$ and $\text{As}_{50}\text{Se}_{50}$. The addition of 10% of As in place of Se into $\text{As}_{40}\text{Se}_{60}$ makes significant change in the parameters like transmission, refractive index, absorption coefficient, optical band gap, τ_{auc} parameter, Urbach energy. The presence of localized states affects the properties of these films with great extent. Information on the degree of disorderness in these materials draws important optical properties change.

All the observed optical properties change are irreversible in nature for which such type of compounds are useful for optical elements that needs high changes with external stimuli. By taking suitable chalcogenide alloys with different gaps, the optical properties can be tuned for optical recording.

Experimental

Materials details

High purity As and Se (99.999 % pure) were purchased from Sigma-Aldrich Chemical Co. Merck KGaA) and used as received.

Material synthesis

The exact proportions according to the atomic percentages of As and Se powder were weighed by a digital electronic weighing balance. The weighed chemical was sealed at evacuated condition ($\sim 10^{-5}$ Torr) inside ampoule made of quartz with length ~ 15 cm and internal diameter ~ 1 cm. After that the sealed ampoule was heated to 1000°C and was constantly rotated for obtaining a homogeneous mixture. The melt was suddenly cooled in ice cooled water after 24h of heating. The ampoule was then broken to take out the formed glassy sample.

The thin film of $\text{As}_{40}\text{Se}_{60}$ and $\text{As}_{50}\text{Se}_{50}$ was prepared from the prepared bulk samples by using thermal evaporation method (Vacuum coating unit 12A4D). The glass substrates of size $1\text{ cm} \times 1\text{ cm}$ were used for the deposition of the films and the base pressure was $\sim 1 \times 10^{-5}$ Torr. The substrates were cleaned properly with acetone before using. The room temperature condition was maintained during the film preparation and the rate of deposition was adjusted at 2 nm/s . The substrates were rotated at low speed during the deposition process for getting homogenous and smooth film. The thickness of the prepared films was $\sim 800\text{ nm}$ as measured by a quartz crystal monitor attached with the coating unit during evaporation process.

Characterizations

The amorphous structure of the prepared films was confirmed from the X-ray (Philips type 1710 with Cu as target and Ni as filter, $\lambda=1.5418\text{ \AA}$) Diffractometer (XRD). The elemental composition of the studied films were checked by using Energy Dispersive X-ray analysis (EDAX) instrument (Sirion XL 40). The scanning of the films was done with 20 kV voltage and $40\text{ }\mu\text{A}$ emission current at pressure of 2×10^{-7} Torr with a sample size of 1 cm^2 . The calculated error was less than 3 % in atomic fraction in each element (**Table 1**). The optical transmission spectra of the two samples were recorded from the Bruker made FTIR spectrometer (Bruker Optics (IFS66v/S) in the wavelength range $500\text{-}1200\text{ nm}$.

The XPS measurement for the two films was done for the bonding information. The core XPS spectra

were recorded by using monochromatic Mg K α X-rays (1253.6 eV) at high vacuum of 10^{-9} Torr (Multilab 2000 Thermo Scientific UK instrument). The selected core level peaks were recorded with energy increment of 1 eV and 0.05 eV for the survey scan over entire binding energy range. The retarding potential with pass energy of 30 eV was used for collecting the core level spectra. The data were collected at different portions of the film for checking the reproducibility. As the charging effect affects the binding energy of the electrons in samples for insulators like glass substrates, the BE measurement of electrons from a specified energy level is not reliable. So, the charge correction was done usually by the C 1s line from either adventitious carbon or intentionally added graphite powder on the surface of the sample. For the present analysis, C 1s BE line was set as 284.6 eV obtained from the adventitious carbon. The recorded original BE data were corrected by the calibration factor which is the difference between the measured C 1s BE and the reference value 284.6 eV [23]. All the data collection was done at room temperature ($\sim 300\text{ K}$).

Results and discussion

XRD Study

The **Fig. 1** shows the X-ray diffraction patterns which is measured at room temperature. The amorphous nature of the studied $\text{As}_{40}\text{Se}_{60}$ and $\text{As}_{50}\text{Se}_{50}$ thin films is confirmed from the absence of sharp structural peaks. The width of broad hump was from 20° - 35° . As the two spectra are very similar to each other, it is not possible to make any difference between the two films.

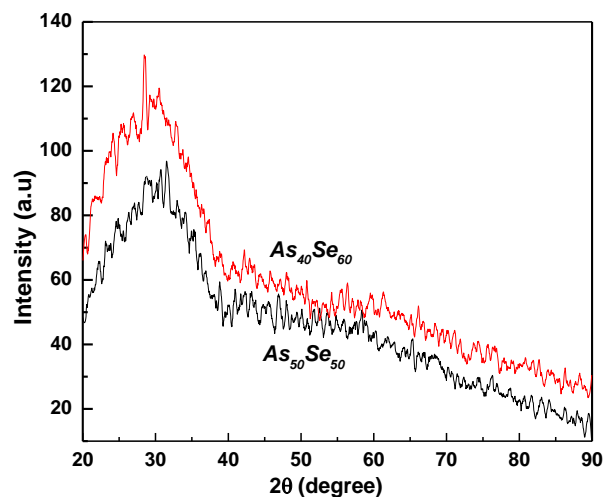


Fig. 1. XRD pattern of for $\text{As}_{40}\text{Se}_{60}$ and $\text{As}_{50}\text{Se}_{50}$ thin films.

EDAX analysis

The composition of the two prepared films were checked by EDAX analysis which showed that their compositions are very near to the starting materials [**Table 1**]. The presence of the elements As and Se is shown in **Fig. 2**. The variation in the composition is within the error limit of 5%.

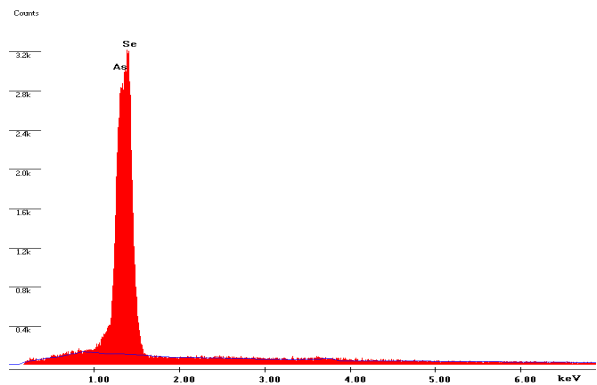


Fig. 2. EDAX spectrum of $As_{50}Se_{50}$ thin film.

Table 1. The measured elemental composition from EDAX for $As_{40}Se_{60}$ and $As_{50}Se_{50}$ thin film.

$As_{40}Se_{60}$				
Element	Wt %		At%	
	Observed	Calculated	Observed	Calculated
As	37.27	38.74	38.65	40
Se	62.73	61.26	61.35	60
Total	100.00	100.00	100.00	100.00
$As_{50}Se_{50}$				
Element	Wt %		At%	
	Observed	Calculated	Observed	Calculated
As	47.31	48.68	49.16	50
Se	52.69	51.32	50.84	50
Total	100.00	100.00	100.00	100.00

FTIR analysis

The Fig. 3 presents the transmission spectra of the $As_{40}Se_{60}$ and $As_{50}Se_{50}$ films from which the optical constant were calculated. The uniformity of the prepared films is confirmed from the appearance of oscillatory interference fringes. The value strength of transmission is found to be increased with wavelength for both $As_{40}Se_{60}$ and $As_{50}Se_{50}$ thin films. Transmittance of $As_{40}Se_{60}$ thin film varies with interference pattern from 50% to 85% in the wavelength range 600nm to 1200nm which shows high values of transmission in the film. But the transmittance of $As_{50}Se_{50}$ thin film varies from 45% to 75% as shown in Fig. 3. So, the addition of more As (10%) into $As_{40}Se_{60}$ decreases the transmission.

The well-known Swanepoel method is used to determine the value of refractive index from the transmission spectrum [21]. The corresponding equation for the refractive index (n) is given by

$$N = [M + (M^2 - S^2)^{1/2}]^{1/2} \tag{1}$$

$$\text{where } M = [2S(T_M - T_m / T_M T_m)] + (S^2 + 1) / 2 \tag{2}$$

T_M and T_m are the maxima and minima of the transmission curve at a particular wavelength, S is the refractive index of the glass substrate (1.51).

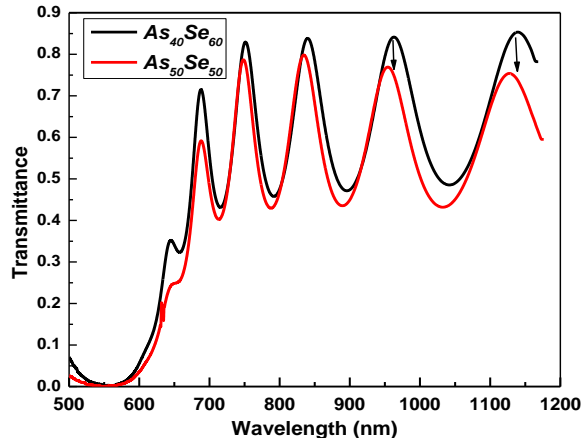


Fig. 3. Transmission spectra of $As_{40}Se_{60}$ and $As_{50}Se_{50}$ thin films.

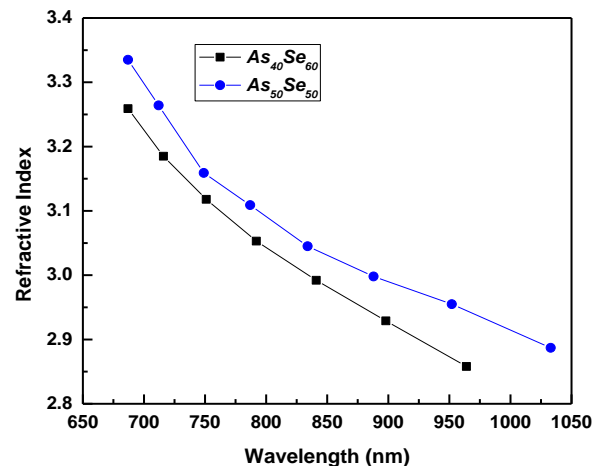


Fig. 4. Variation of refractive index in $As_{40}Se_{60}$ and $As_{50}Se_{50}$ thin films.

The fringes at different wavelength are being used for calculating the refractive index by extrapolating envelopes corresponding to T_M to T_m . The refractive index is found to decrease with the increase in wavelength and increases with As addition as shown in Fig. 4. Refractive index is increased for $As_{50}Se_{50}$ due to local structural modification which brings the As & Se atoms close to each other. The bond angle and bond length changes due to the As addition.

The absorption coefficient (α) can be calculated using the equation [24]

$$\alpha = \frac{1}{d} \ln \left(\frac{(1-R)^2}{T} \right) \tag{3}$$

where d is thickness of thin film, T is transmission and R is the reflection. The absorption coefficients (α) vs wavelength (λ) for both the films are shown in the Fig. 5. The absorption coefficient is the measure of the loss by absorption and scattering phenomena in the electromagnetic wave propagation through the medium. The gradual reduction of α with λ infers the more transparency of the material at higher wavelength which is useful for making optical material. The transition between valence band and conduction band is associated with the fundamental edge that determines direct and indirect the band gaps in crystalline material. Due to the absence of particular electronic band

structure in k space for amorphous materials, the band gap is no-direct one. Generally, the absorption edge is due to the excitation of electrons from lower to higher energy state by photon energy. The value of α is found to be increased for the $As_{50}Se_{50}$ than the $As_{40}Se_{60}$ film.

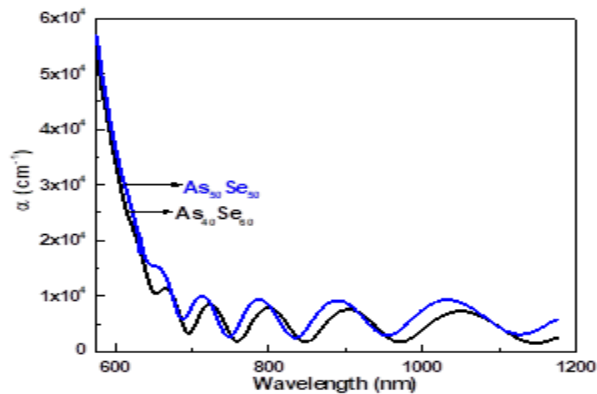


Fig. 5. Absorption coefficient of $As_{40}Se_{60}$ and $As_{50}Se_{50}$ thin films.

The fundamental absorption edge follows an exponential behavior in many amorphous semiconductors which is the most productive tool for the formulation of energy band diagram. The Tauc relation which follows an exponential behaviour in amorphous semiconductors in the high absorption region ($\alpha > 10^4 \text{ cm}^{-1}$) is given by [25]

$$(\alpha h\nu)^{1/m} = B^{1/m} (h\nu - E_g) \quad (4)$$

where ν is the frequency, B is tauc parameter, E_g is the band gap and m is an exponent number having values such as 1/2, 3/2, 2 and 3 for allowed direct, forbidden direct, allowed indirect and forbidden indirect transition respectively [26]. The non-direct allowed transition is happening in both the $As_{40}Se_{60}$ and $As_{50}Se_{50}$ thin films as the best fit is found with the value of $m=1/2$ as shown in the variation curve of $(\alpha h\nu)^{1/2}$ with $h\nu$ (Fig. 6). The dependence of $(\alpha h\nu)^{1/2}$ vs $(h\nu)$ gives a straight line and the y intercept gives the value of the optical band gap as shown in Fig. 6.

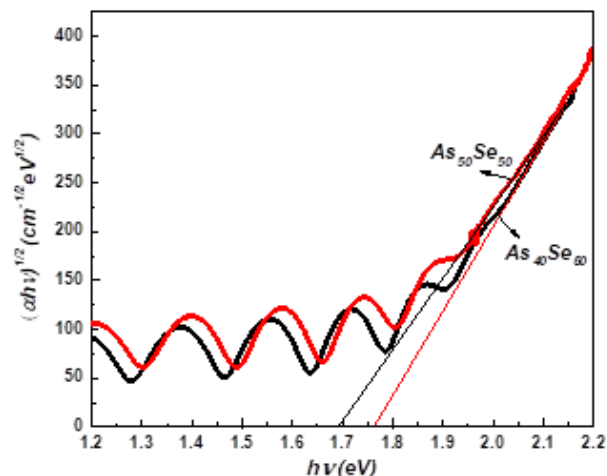


Fig. 6. $(\alpha h\nu)^{1/2}$ vs $(h\nu)$ plots for the $As_{40}Se_{60}$ and $As_{50}Se_{50}$ thin films.

The E_g of the $As_{40}Se_{60}$ and $As_{50}Se_{50}$ films are found to be $1.76 \pm 0.001 \text{ eV}$ and $1.69 \pm 0.001 \text{ eV}$ respectively. The E_g of $As_{50}Se_{50}$ film is found to be reduced by 0.07 eV from the $As_{40}Se_{60}$ film which shows the reduction of band gap in the film. The "density of state model" proposed by Mott and Davis [27] is used for explaining the decrease in E_g as the optical absorption depends on the short-range order in the amorphous states and defects associated with it. The degree of disorder and defect states determines the width of the localized states near the mobility edges of the amorphous structure according to the model. It also states that unsaturated bonds along with some saturated bonds are produced due to the deposition of insufficient number of atoms in the film.

The localized states in amorphous materials are formed due to the presence of such type of unsaturated bonds that causes the origin of defect states in the film. The lowering of band gap is mainly due to the formation of high amount of such localized states in the band structure. Another reason for the reduction of optical band gap is due to the variation of the position of Fermi level and the electron distribution over the localized states evaluates the position of fermi level [28]. The decrease of density of tail near to the band edge causes the decrease of E_g with addition of As. This causes the increase in homopolar bonds like As-As and Se-Se bond density and decreases the structural ordering. In generally, the reduction of E_g (red shift in the absorption edge) is accompanied by the simultaneous increase in the value of n according to Moss's rule ($E_g n^4 \sim \text{constant}$) [29] which is seen in Fig. 4.

The $B^{1/2}$ parameter is obtained from the slope of the fitting in eqn. 4 that gives the information about the convolution of the two bands valence band and conduction band. This is a very useful constant that gives the k selection rule and optical transition due to the disorder induced spatial correlation [30]. The tauc parameter is highly dependent on the character of the bonding [31]. The values of $B^{1/2}$ for $As_{40}Se_{60}$ and $As_{50}Se_{50}$ films are found to be 763 and $683 \text{ cm}^{-1/2} \text{ eV}^{-1/2}$ respectively. This decrease in tauc parameter indicates that the value of E_g is reduced by the increase of disorderness due to which the band tail extends into the gap region. The lowering of $B^{1/2}$ with E_g indicates the presence of large no of homopolar bonds in the $As_{50}Se_{50}$ film.

In chalcogenide system, the optical edge is reproducible because they are relatively insensitive for preparation conditions. The observable absorption mechanism with a gap under equilibrium conditions is responsible for such process. For this reason, a different type of optical absorption edge is found in amorphous materials and the α value increases exponentially with $h\nu$ near the energy gap. Such type of optical absorption edge is known as the Urbach edge that gives information regarding the degree of disorderness and denoted by [32]

$$\alpha(h\nu) = \alpha_0 \exp\left(\frac{h\nu}{E_e}\right) \quad (5)$$

where α_0 is a constant (absorption coefficient at optical band gap) and E_e corresponds to the Urbach energy. This parameter is a measure of the width of the band tail of the localized states in the band gap. The equation 5 shows the absorption process of the amorphous materials in frequency range ($10^0 < \alpha < 10^4 \text{ cm}^{-1}$) where transition between (defect) states in the gap and the bands take place [33]. The graph between $\log(\alpha/\alpha_0)$ vs $(h\nu)$ gives a straight line and the inverse of the slope obtained measures E_e . Urbach energy E_e is a very useful parameter to evaluate the degree of structural disorder in the film [34]. The value of E_e for $\text{As}_{40}\text{Se}_{60}$ and $\text{As}_{50}\text{Se}_{50}$ film is 91 meV and 168 meV respectively. The higher values of E_e of the $\text{As}_{50}\text{Se}_{50}$ film over $\text{As}_{40}\text{Se}_{60}$ film clearly infers that $\text{As}_{50}\text{Se}_{50}$ film is more structurally disordered than $\text{As}_{40}\text{Se}_{60}$ film, which might be due to the creation of homopolar bonds after 10% addition of As.

Although the XPS spectrum of $\text{As}_{40}\text{Se}_{60}$ and $\text{As}_{50}\text{Se}_{50}$ film contains many photoelectrons and Auger peaks of As and Se but, we have analyzed Se 3p and As 3d core peaks for the present study. The fig. 7 shows the Se 3d and As 3d spectra of the $\text{As}_{40}\text{Se}_{60}$ and $\text{As}_{50}\text{Se}_{50}$ films in which As 3d peak for the $\text{As}_{40}\text{Se}_{60}$ film is at 43.08 eV that shifts to 42.67 eV for $\text{As}_{50}\text{Se}_{50}$ thin film. This change of 0.41 eV towards lower energy side infers the formation of more As-As bonds due to As addition. The BE of the Se 3d peak for $\text{As}_{40}\text{Se}_{60}$ film is at 55.29 eV which moves to 54.73 eV with As addition by decreasing Se%. Due to the addition of As into $\text{As}_{40}\text{Se}_{60}$ matrix, large amount of Se-Se bonds are formed which can be noticed from the shift of Se 3d peak. The formation of large no of homopolar bonds like As-As and Se-Se instead of As-Se heteropolar bond, increases the disorderness in the film. This extra amount of homopolar bonds in $\text{As}_{50}\text{Se}_{50}$ film can modify the local microstructure and grain morphology leading to the increase in film packing density and that increases the refractive index.

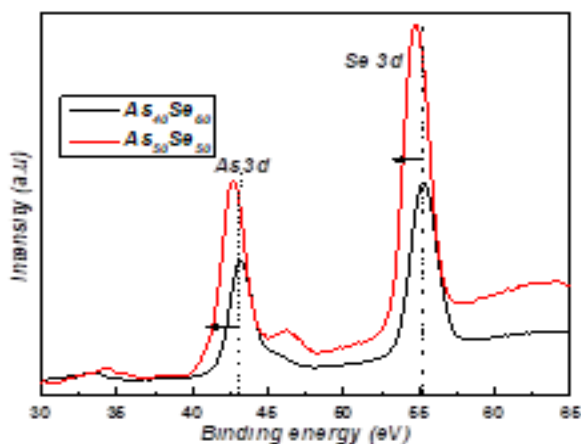


Fig. 7. XPS core level As 3d and Se 3d spectra for the $\text{As}_{40}\text{Se}_{60}$ and $\text{As}_{50}\text{Se}_{50}$ thin films.

Conclusion

The addition of more As into $\text{As}_{40}\text{Se}_{60}$ alloy changes the optical properties to great extent without changing the structural property. The transmission % is reduced with 10% of As whereas the absorption coefficient increases. The indirect allowed transition for the absorption process decreases the optical band gap with As addition as a result of increased band tailing. The degree of disorder measured by the Tauc parameter and Urbach energy shows the changes between $\text{As}_{40}\text{Se}_{60}$ and $\text{As}_{50}\text{Se}_{50}$ film. The width of localized states increases with the incorporation of As content thus decreasing the optical band gap. The formation of more homopolar bonds for which the reduction of optical band gap occurs is reflected from the shift in BE of core level XPS peaks. These optical constants change can be used to design specific types of optoelectronic and integrated optical elements that requires high local changes of optical constants.

Acknowledgements

The authors thank Department of Science and Technology (DST), Govt of India for DST-INSPIRE Research grant and using the National Facility for Optical Spectrometry at Department of Physics and Surface Science facility, Indian Institute of Science (IISc) for XPS measurement.

Author's contributions

Conceived the plan: R.Naik; Performed the experiments: C. Sripan; Data analysis: R.Naik and R. Ganesan; Wrote the paper: R. Naik. Authors have no competing financial interests.

References

- Lankhorst, M.H.R; *Nat. Mater.*; **2005**, *4*, 347.
DOI: [10.1038/nmat1350](https://doi.org/10.1038/nmat1350)
- Wang, F; Zhang, Z; Liu, R; Wang, X; Zhu, X; Pan, A; Zou, B; *Nanotechnology*, **2007**, *18*, 305705.
DOI: [10.1088/0957-4484/18/30/305705](https://doi.org/10.1088/0957-4484/18/30/305705)
- Marquez, E; Gonzalez-Leal, J. M; Jimenez-Garay, R; Vlcek, M; *Thin Solid Films*, **2001**, *396*, 183.
DOI: [10.1016/S0040-6090\(01\)01219-6](https://doi.org/10.1016/S0040-6090(01)01219-6)
- R. Naik; *Adv. Mat. Lett.* **2016**, *7*(10), 150.
DOI: [10.5185/amlett.2016.6339](https://doi.org/10.5185/amlett.2016.6339)
- Zakery, A; Elliot, S.R; *J. Non-Cryst. Solids*, **2003**, *330*, 1.
DOI: [10.1016/j.jnoncrysol.2003.08.064](https://doi.org/10.1016/j.jnoncrysol.2003.08.064)
- R. Naik; A. Jain; R. Ganesan; K.S.Sangunni; *Thin Solid Films*, **2012**, *520*, 2510.
DOI: [10.1016/j.tsf.2011.10.029](https://doi.org/10.1016/j.tsf.2011.10.029)
- M. Behera, R. Naik, *Appl. Phys. A*, **2016**, *122*, 913
DOI: [10.1007/s00339-016-0451-7](https://doi.org/10.1007/s00339-016-0451-7)
- J. Vazquez; C. Wagner; P. Villares; *J. Non-Cryst. Solids*, **1998**, *235*, 548.
DOI: [10.1016/S0022-3093\(98\)00661-9](https://doi.org/10.1016/S0022-3093(98)00661-9)
- J. George; M.K. Radhakrishnan; *Solid State Commun.* **1980**, *33*, 987
DOI: [10.1016/0038-1098\(80\)90296-3](https://doi.org/10.1016/0038-1098(80)90296-3)
- B. Roy; B.R. Chakraborty; R. Bhattacharya; A.K. Dutta; *J. Phys. Chem. Solids*, **1980**, *41*, 913.
DOI: [10.1016/0022-3697\(80\)90037-2](https://doi.org/10.1016/0022-3697(80)90037-2)
- R.J. Nemanich; G.A. Connel; T.M. Haynes; R.A. Street, *Phys. Rev. B*, **1978**, *18*, 6900
DOI: [10.1103/PhysRevB.18.6900](https://doi.org/10.1103/PhysRevB.18.6900)
- Kolobov A V 2003 *Photo-induced Metastability in Amorphous Semiconductors* (Berlin: Wiley-VCH)
ISBN: [978-3-527-60866-9](https://doi.org/10.1002/978-3-527-60866-9)
- R. Naik, *Adv. Mater. Lett.* **2015**, *6*(6), 531.
DOI: [10.5185/amlett.2015.5753](https://doi.org/10.5185/amlett.2015.5753)

14. T. Zhao, S. Lou, W. Su, X. Wang, *J. Mod. Optice*, **2016**, 63, 139.
DOI: [10.1080/09500340.2015.1071884](https://doi.org/10.1080/09500340.2015.1071884)
15. Y. Tang, F. Li, J. Xu, *Laser Phys.* **2016**, 26, 055402
DOI: [10.1088/1054-660X/26/5/055402](https://doi.org/10.1088/1054-660X/26/5/055402)
16. Krecmer P; Moulin A M; Stephenson R J; Rayment T, Welland M E; Elliott S R, *Science*, **1997**, 277, 1799
DOI: [10.1126/science.277.5333.1799](https://doi.org/10.1126/science.277.5333.1799)
17. Frumar M, Frumarova B, Nemeč P,Wagner T, Jedelsky J and Hrdlicka M, *J. Non-Cryst. Solids*, **2006**, 352, 544-561.
DOI: [10.1016/j.jnoncrysol.2005.11.043](https://doi.org/10.1016/j.jnoncrysol.2005.11.043)
18. Frumar M; Jedelsky J; Frumarova B; Wagner T; Hrdlicka M , *J. Non-Cryst. Solids*, **2003**, 326-327, 399
DOI: [10.1016/S0022-3093\(03\)00446-0](https://doi.org/10.1016/S0022-3093(03)00446-0)
19. B J Eggleton; B Luther-Davies; K Richardson, *Nat. Photonics*, **2011**, 5, 141.
DOI: [10.1038/nphoton.2011.309](https://doi.org/10.1038/nphoton.2011.309)
20. A B Seddon; *J. Non-Cryst. Solids*, **1995**, 184, 44.
DOI: [10.1016/0022-3093\(94\)00686-5](https://doi.org/10.1016/0022-3093(94)00686-5)
21. Swanepoel R; *J. Phys. E: Sci. Instrum.* **1983**, 16, 1214.
DOI: [10.1088/0022-3735/16/12/023](https://doi.org/10.1088/0022-3735/16/12/023)
22. R. Naik; S. Jena; R. Ganesan; N. K.Sahoo, *Laser Phys.*, **2015**, 25, 036001.
DOI: [10.1088/1054-660X/25/3/036001](https://doi.org/10.1088/1054-660X/25/3/036001)
23. T. L. Barr; S. Seal; *J. Vac. Sci. Technol. A*, **1995**, 13, 1239.
DOI: [10.1116/1.579868](https://doi.org/10.1116/1.579868)
24. A.A. Othman; M.A. Osman; H.H. Amer; A. Dahshan; *Thin Solid Films*, **2004**, 457, 253.
DOI: [10.1016/j.tsf.2003.10.158](https://doi.org/10.1016/j.tsf.2003.10.158)
25. Tauc, J.; *Amorphous and liquid semiconductor*,(New York, Plenum Press). **1974**,179.
ISBN: 0-306-307774
26. R.Naik; S. Jena; R. Ganesan; N. K. Sahoo; *Physica Status Solidi B*, **2014**, 251, 661
DOI: [10.1002/pssb.201350060](https://doi.org/10.1002/pssb.201350060)
27. Mott, N.F.; Davis, E.A.;*Electronic process in Non-crystalline Materials*, Clarendon: Oxford, **1979**, 382.
ISBN: 10: 0198512880
28. Nang, T. T.; Okuda, M.;Matsushita,T.; Yakota, S.; Suzuki, A.; *Jap. J. Appl. Phys.*, **1976**, 15, 849.
DOI: [10.1143/JJAP.15.849](https://doi.org/10.1143/JJAP.15.849)
29. Knotek, P.; Tichy, L.; Arsova, D.; Ivanova, Z. G.; Ticha, H.; *Mater. Chem. Phys.*, **2010**, 119, 315
DOI: [10.1016/j.matchemphys.2009.09.003](https://doi.org/10.1016/j.matchemphys.2009.09.003)
30. A.R. Zanatta, I. Chambouleyron, *Phys. Rev. B*, **1996**, 53, 3833.
DOI: [10.1103/PhysRevB.53.3833](https://doi.org/10.1103/PhysRevB.53.3833)
31. J.D. Dow, D. Redfield, *Phys. Rev. B*, **1970**, 1, 3358 .
DOI: [10.1103/PhysRevB.1.3358](https://doi.org/10.1103/PhysRevB.1.3358)
32. Urbach, F.; *Phys. Rev.* **1953**, 92, 1324.
DOI: [10.1103/PhysRev.92.1324](https://doi.org/10.1103/PhysRev.92.1324)
33. Elliot, S.R.; *The Physics and Chemistry of Solids*, John Wiley & Sons: UK, **1998**.
ISBN: 0471981958
34. Cody, G.D.; Tiedje, T.; Abeles, B.; Brooks, B.; Goldstein, Y.; *Phy. Rev. Lett.* **1981**, 47, 1480.
DOI: [10.1103/PhysRevLett.47.1480](https://doi.org/10.1103/PhysRevLett.47.1480)